nature portfolio

Peer Review File

Origin of charge density wave in topological semimetals SrAl4 and EuAl4

Reviewers' comments:

Reviewer #1 (Remarks to the Author):

The paper discusses the origin of the charge density wave (CDW) in SrAl4 and EuAl4, providing a comprehensive theoretical study using density functional theory. The content is of high quality and certainly worthy of publication. However, there are certain issues and questions that need to be addressed by the authors in order to publish this paper.

The manuscript refers to the existence of surface states in the materials discussed. However, the mere presence of these surface states doesn't necessarily guarantee that they are non-trivial topological in nature. More detailed analysis is needed to confirm the topological nature of these states. I suggest that the authors elaborate on the methods used to identify these states as topological. This may require additional calculations, including wave function analysis, spin texture, and topological invariants, or a discussion of the methods used.

The susceptibility calculations are central to the results presented. I found that the paper could benefit from more explicit details of these calculations. In particular, the process by which the authors evaluated the susceptibility should be more fully explained in the methods section. The manuscript mentions both the real (Re) and imaginary (Im) parts of the susceptibility function. For readers, and especially for those who may not be directly familiar with this particular methodology, an explanation of the physical implications of these components would be beneficial. In addition, the interpretation and meaning of the peaks seen in the susceptibility functions should be further explained. In some parts, changes were noted in the susceptibility functions, either in the real or imaginary parts. There were cases where peak shifts were observed. It would be beneficial for the authors to provide a more comprehensive analysis of the significance of these shifts and changes. In particular, how do these changes correlate with the presence of CDW states and other instabilities? This would add depth to the discussion and strengthen the results presented.

Reviewer #2 (Remarks to the Author):

In this manuscript, the authors performed the first-principle studies on the driving force of CDW in SrAl4 and EuAl4. According to their results, the large electron-phonon coupling and fermi surface nesting is the driven force of the CDW.

I noticed another experimental and theoretical work on CDW in SrAl4 appeared on arxiv(2309.08959). According to their conclusion, small imaginary frequencies were due to the insufficient k-points sampling. In this situation, I would ask the authors to proof the reliability of their works first, and then I could make my decision.

Reviewer #3 (Remarks to the Author):

In the manuscript by Wang, Nepal and Canfield, the authors theoretically investigate the origins of the CDW in SrAl4 and EuAl4. They calculate the electronic and phonon bandstructure using first principles and then investigate the susceptibility functions using maximally localized Wannier functions. To understand the origins of the CDW, they consider related compounds, in particular BaAl4, that have similar crystal structure and bandstructure but no CDW. The authors find there is an enhanced electron-phonon coupling to a transverse acoustic phonon in SrAl4 and EuAl4 and a peak in the real part of the susceptibility function at the experimentally observed CDW q-vector. The authors conclude this is a stronger driving force towards the formation of the CDW than a Peierls distortion arising from imperfect Fermi surface nesting.

The manybody interactions in topological systems is a contemporary topic that appeals to a wide audience and is suitable for publication in Communication Physics. The theoretical investigation is thorough, and the conclusions are well grounded. However, I do have one concern that should be addressed prior to recommending for publication.

The authors discuss conventional wisdom and what one should expect from the replacement of Sr with the more massive Ba ions. In summary, one should expect that $BaAl_4$ should also form a CDW due to the heavier Ba ions. The authors then discuss how the Ba compound does not follow conventional wisdom as the electron-phonon coupling is reduced for the TA phonon responsible for the CDW formation and hence, does not exhibit a CDW. While I agree with these conclusions, I am still left wondering why. As the authors point out, the electron phonon coupling interaction has no mass dependence but evaluates changes to the deformation potential. Hence, what are these differences that deviates the behavior from the conventional wisdom. Do subtle crystal changes from the different cation sizes result in an alteration of the deformation potential observed by the electrons? Do the bulked nets of Al get altered by the different cations? If it is driven by the enhancement of the electronic phonon coupling, what is driving this enhancement? In other words, what updates to conventional wisdom can we draw from these results?

Reviewer #1 (Remarks to the Author):

The paper discusses the origin of the charge density wave (CDW) in SrAl4 and EuAl4, providing a comprehensive theoretical study using density functional theory. The content is of high quality and certainly worthy of publication. However, there are certain issues and questions that need to be addressed by the authors in order to publish this paper.

REPLY: We thank the reviewer for the careful reading of our manuscript and finding our work to be comprehensive and in high quality.

The manuscript refers to the existence of surface states in the materials discussed. However, the mere presence of these surface states doesn't necessarily guarantee that they are non-trivial topological in nature. More detailed analysis is needed to confirm the topological nature of these states. I suggest that the authors elaborate on the methods used to identify these states as topological. This may require additional calculations, including wave function analysis, spin texture, and topological invariants, or a discussion of the methods used.

REPLY: We thank the reviewer's suggestion for expanding the discussion on topological analysis of the band structure of SrAl4 in Fig.1. Firstly, from the symmetry of the bulk bands, the space group 139 (I4/mmm) has inversion symmetry. When combining with time-reversal symmetry, every band is doubly degenerated even with spin-orbit coupling (SOC). We have calculated the wavefunctions at the high-symmetry k-points and analyzed them using Vasp2trace [Ref.38 and 39, Vergniory et al], which constructs elementary band representation (EBR) of the bulk bands from high-symmetry k-points and Wycoff sites to analyze topological invariants and symmetry-protected band crossings. Such method is also called topological quantum chemistry [Ref.45, Bradlyn et al] and is equivalent to the symmetry-based indicators [Ref.41, Po et al], layered construction [Ref.44, Song et al] and also other related methods [Ref.42, Slager et al and Ref.43, Kruthoff et al]. The point group symmetry is D4h. From the double group representation of D4h for the spinful system, the top valence band along the Γ-Z direction with the 4-fold rotation switches between two different 2-dimensioinal irreducible representations of Λ7 and Λ6, thus there is no mixing guarantied at the band crossing, or equivalently speaking, the Dirac point (DP) is protected by the 4-fold rotational symmetry [Ref.40, Yang et al]. We have labeled the irreducible representations of Λ7 and Λ6 for the two crossing bands as zoomed in Fig.1(d) along the Γ-Z direction. Our results also agree with the earlier paper [Ref.22, Wang et al] that already analyzed the topological nature of the DPs and the irreducible representations in BaAl4.

Secondly, we have constructed the tight-binding Hamiltonian using the maximally localized Wannier functions, which reproduces very well the bulk band structure in the range of EF+/-1 eV. We then used the tight-binding Hamiltonian to search throughout the whole Brillouin zone (BZ) to confirm that the pair of DP along the Γ-Z direction (+/-kz) are the only band crossings between the highest valence band and lowest conduction band. Using DFT calculation directly, we also zoomed in Fig.1(d) along the kz to verify the zero gap and the switching of the different orbital characters at the DP, which provide

the evidence for the non-mixing of these two crossing bands at the DP due to the two different irreducible representations. In contrast, along other directions without the 4-fold rotation, the two crossing bands can mix to form a mass term because SOC gaps out the nodal loops, which is confirmed by the thorough search with the tight-binding Hamiltonian using Wannier functions.

Thirdly, the two surface states (SS) in Fig.1(f) converge to the projection of the DPs on (001) surface. We have added the spin-texture in panel (g) to show that these SS are spin-momentum locked as expected for non-trivial topological SS. There are two SS because of the projection of two DPs at +/-kz onto the same $\bar{\Gamma}$ point on (001). Furthermore, we have included these topological SS in the other direction of $\bar{\Gamma}$-$\bar{M}$ with quite different band dispersion, but still they converge to the same DP projection, which are from the only pair of conical points between the highest valence and lowest conduction bands.

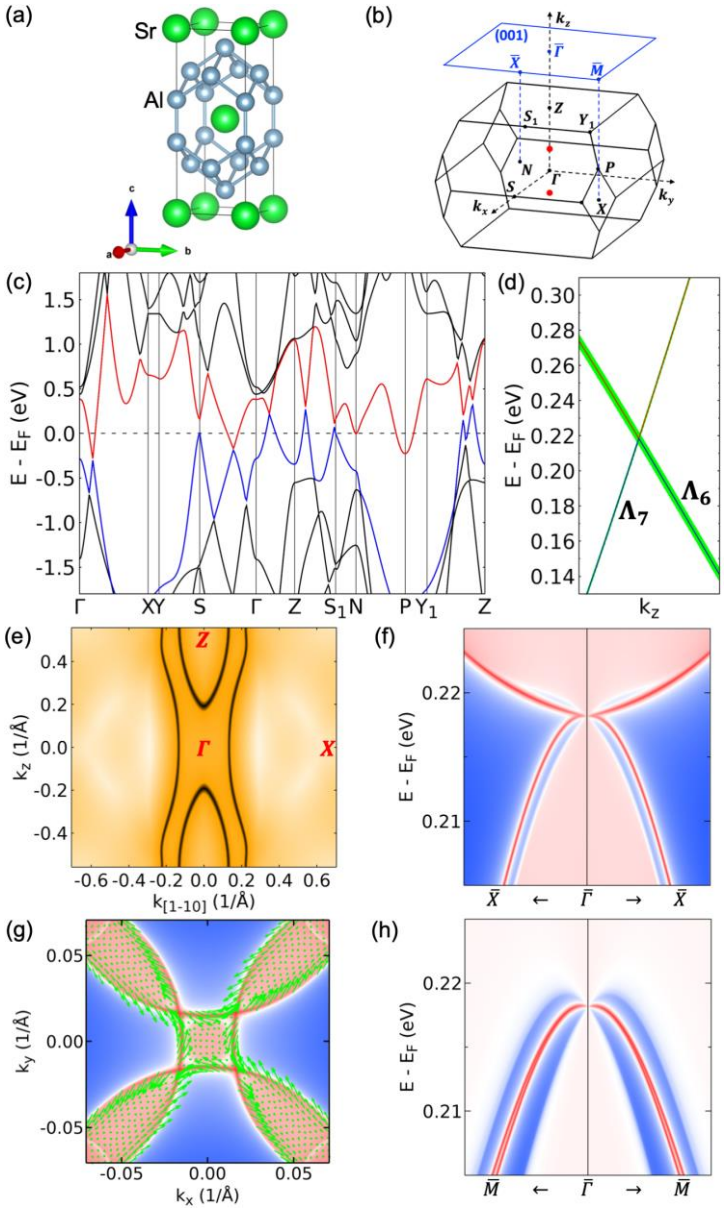

Thus, we have added the following discussion of the topological analysis of the band structure in the main text.

"The point group symmetry is D_{4h}. We have used Vasp2trace[38, 39] to analyze the elementary band representations. From the double group representation of D_{4h} for the spinful system, the top valence band along the Γ-Z direction with the 4-fold rotation switches between two different 2-dimensioinal irreducible representations of Λ_7 and Λ_6, thus there is no mixing guarantied at the band crossing, or equivalently speaking, the pair of Dirac points (DPs) is protected by the 4-fold rotational symmetry[40-45]. Our results also agree with the previous study[22] on $BaAl_4$ for the DPs along the Γ-Z direction."

The susceptibility calculations are central to the results presented. I found that the paper could benefit from more explicit details of these calculations. In particular, the process by which the authors evaluated the susceptibility should be more fully explained in the methods section. The manuscript mentions both the real (Re) and imaginary (Im) parts of the susceptibility function. For readers, and especially for those who may not be directly familiar with this particular methodology, an explanation of the physical implications of these components would be beneficial. In addition, the interpretation and meaning of the peaks seen in the susceptibility functions should be further explained. In some parts, changes were noted in the susceptibility functions, either in the real or imaginary parts. There were cases where peak shifts were observed. It would be beneficial for the authors to provide a more comprehensive analysis of the significance of these shifts and changes. In particular, how do these changes correlate with the presence of CDW states and other instabilities? This would add depth to the discussion and strengthen the results presented.

REPLY: We thank the reviewer's suggestion. The susceptibility function here, $\chi(\boldsymbol{q})$, is the bare susceptibility function based on DFT single-particle Kohn-Sham bands, as described for example in Ref.14 [Johannes and Mazin, PRB 77, 165135 (2008)]. We have expanded the discussion and provided the formula for the real and imaginary parts of $\chi(\boldsymbol{q})$ in the main text, and also given details of the calculation in the Methods section. Please also find below.

"To study FSN and CDW from band structure, the bare susceptibility function[14], $\chi(\boldsymbol{q})$, based on DFT single-particle Kohn-Sham bands needs to be calculated in real and imaginary parts,

$$Re\chi(\boldsymbol{q}) = \sum_{n,m,\boldsymbol{k}} \frac{f(\varepsilon_{n,\boldsymbol{k}}) - f(\varepsilon_{m,\boldsymbol{k}+\boldsymbol{q}})}{\varepsilon_{n,\boldsymbol{k}} - \varepsilon_{m,\boldsymbol{k}+\boldsymbol{q}}} \quad (1)$$

$$\lim_{\omega\to 0} Im\chi(\boldsymbol{q},\omega)/\omega = \sum_{n,m,\boldsymbol{k}} \delta(\varepsilon_{n,\boldsymbol{k}})\delta(\varepsilon_{m,\boldsymbol{k}+\boldsymbol{q}}) \quad (2)$$

where $f(\varepsilon_{n,\boldsymbol{k}})$ and $\delta(\varepsilon_{n,\boldsymbol{k}})$ are the Fermi-Dirac distribution and Delta functions respectively, of $\varepsilon_{n,\boldsymbol{k}}$ the *n*-th band energy eigenvalue at the $\boldsymbol{k}$ point with the E_F set to zero. The calculation of $\chi(\boldsymbol{q})$ requires very dense double meshes ($\boldsymbol{k}$ and $\boldsymbol{q}$). Using the maximally localized Wannier functions (MLWF), we are able to calculate the 3D susceptibility function $\chi(\boldsymbol{q})$ efficiently with millions of $\boldsymbol{k}$-points in the BZ."

"The susceptibility functions in Eqn.(1) and (2) have been calculated with four bands, two valence and two conduction bands, around the E_F on the dense (120×120×90) *k* and *q*-mesh using the MLWFs, where the Fermi-Dirac distribution is sampled at the temperature of 100 K and the Delta functions are approximated with Gaussian functions with a smearing of 0.02 eV."

The shift and different shapes of the peaks in the susceptibility functions have been discussed as imperfect Fermi surface nesting (FSN) for the different compounds in Fig.2 and Fig.3. They correspond to the shift and change of the band structures and Fermi surfaces for BaAl4, SrGa4 and BaGa4 (Fig.3) in comparison to those of SrAl4 (Fig.1(c) and Fig.2(a-c)). We have discussed such differences in the original manuscript,

"The Im$\chi(q)$ of $BaAl_4$ as plotted in Fig.2(e), also has a maximum along the Γ-Z direction, which has a larger *q*-vector and with a more extended plateau than that of $SrAl_4$. In contrast, the Reχ_{max} of $BaAl_4$ in Fig.2(g) is at a smaller *q*-vector than that of $SrAl_4$. This shows a more imperfect FS nesting in $BaAl_4$ than $SrAl_4$ and the mismatch of the peaks in Im$\chi(q)$ and Re$\chi(q)$ is not unexpected, because the latter include contributions from the bands away from the E_F."

We have also added more for EuAl4 in discussion of Fig.5(a-b)). "Noticeably, the Reχ_{max} of EuAl4 has a relatively narrow peak similar to SrAl4 at a small q-vector, rather than the extended plateau of BaAl4."

However, as shown by our analysis of electron-phonon coupling (EPC) for the three Al compounds in Fig.4 and Fig.5, besides the difference among the peaks of the susceptibility functions, the driving force to determine the existence of CDW or not is the different magnitude of the EPC at the small q-vector. Now we have also connected such different CDW behaviors to the different shear modulus and Poisson ratio, which can also be explained well with electron charge density redistributions between the Al network and different cation layers (please also see the replies to Reviewer 3).

Reviewer #2 (Remarks to the Author):

In this manuscript, the authors performed the first-principle studies on the driving force of CDW in SrAl4 and EuAl4. According to their results, the large electron-phonon coupling and fermi surface nesting is the driven force of the CDW.

I noticed another experimental and theoretical work on CDW in SrAl4 appeared on arxiv(2309.08959). According to their conclusion, small imaginary frequencies were due to the insufficient k-points sampling. In this situation, I would ask the authors to proof the reliability of their works first, and then I could make my decision.

REPLY: We thank the reviewer for bringing this arXiv paper to our attention. We have tested the convergence of our phonon calculations for SrAl4 with respect to the k-points

sampling using both DFPT in QE and the finite displacement method in VASP with Phonopy to prove the existence of the imaginary transverse acoustic (TA) mode at the small q-vector as shown in the new Fig.S3 (also below). This imaginary mode with softening of the TA mode at the small q-vector requires highly stringent tolerances for electronic self-consistent iteration and ionic relaxation. For example, our primitive unit cell is relaxed with very high energy and force convergence tolerance of 10^-8 eV and 10^-4 eV/A, respectively, in contrast, the arXiv paper only used the tolerance of 10^-7 eV and 10^-2 eV/A, respectively.

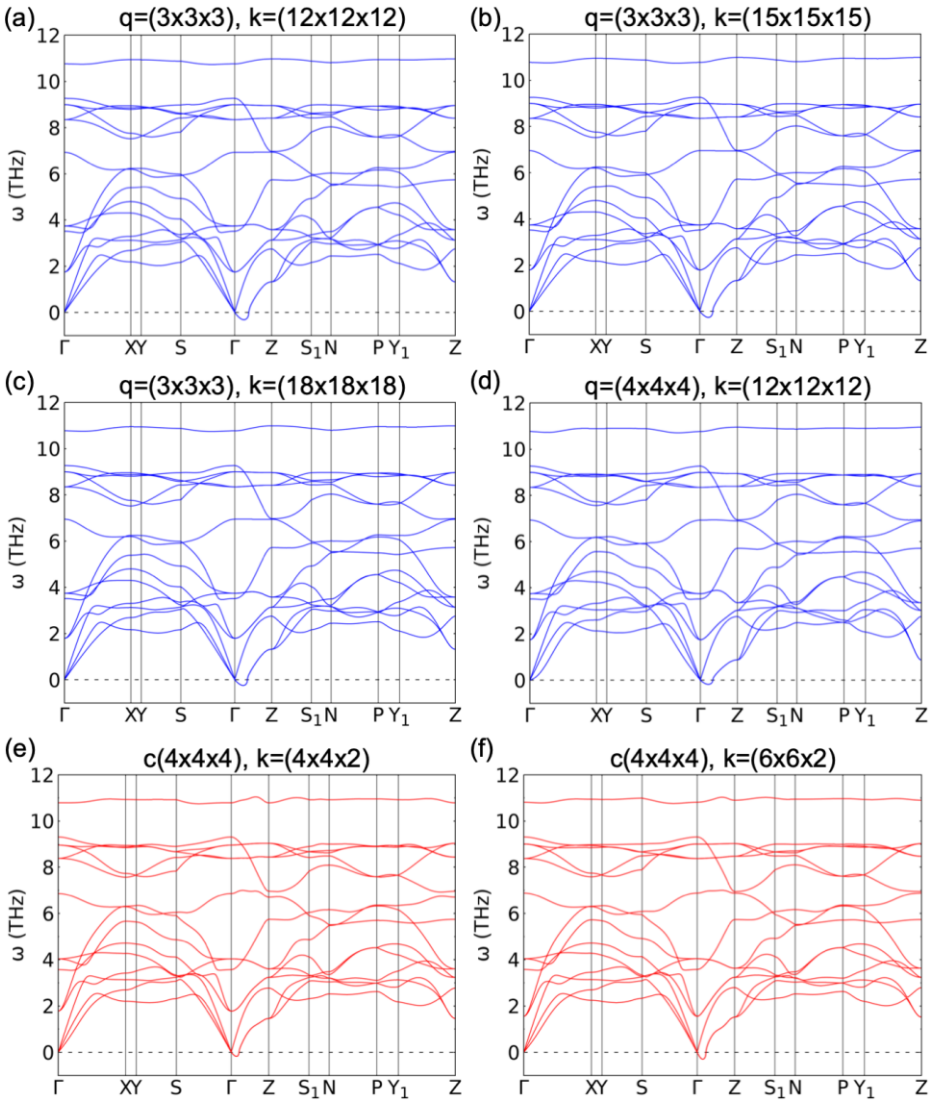

In the arXiv paper, their Fig.6 caption says “DFPT calculations for a 3x3x2 supercell of the conventional unit cell”, but the main text says “3x3x3 supercell of the primitive basic cell, containing 135 atoms”. These descriptions are confusing, because DFPT method should use q-mesh of the primitive cell. Then for the finite displacement method, they used “the same 3x3x3 supercell” with two k-meshes of 3x3x3 and 5x5x5.

For DFPT in QE as shown in Fig.S3 (a)-(d), with the q-mesh of (3x3x3), we have increased the k-mesh from (9x9x9) to (12x12x12), (15x15x15) and (18x18x18) to check the k-mesh convergence. We have also increased the q-mesh from (3x3x3) to (4x4x4) with the k-mesh of (12x12x12) to check the q-mesh convergence. The imaginary TA mode at the small q-vector persists with the different combination of increased k-mesh and q-mesh. In contrast, the arXiv paper only used an equivalent q-mesh of (3x3x3) or (3x3x2) with a k-mesh of (4x4x2) as claimed.

For the finite displacement method, we have already used the (3x3x4) supercell of the conventional cell with 360 atoms in Fig.3. In contrast, the arXiv paper only used a (3x3x3) supercell of the primitive cell with 135 atoms, which is more than two times smaller than our supercell. Because the imaginary TA mode at the small q-vector is along the kz direction, we find it requires a large dimension along the c-axis to accommodate the TA mode with such a small q-vector. Thus, we have chosen the (3x3x4) supercell of the conventional cell, labeled as c(3x3x4), with four time the lattice constant along the c-axis at 45.0 A. For the in-plane direction, the dimension of 13.4 A is also large enough to avoid the interaction between periodic images of the finite displacement in the supercell. To test the size convergence of the supercell, we have increased the size of supercell of the conventional cell from c(3x3x4) of 360 atoms to c(4x4x4) of 640 atoms for a larger in-plane dimension of 17.8 A and also with two different k-mesh of (4x4x2) and (6x6x2) in Fig.S3 (e) and (f), respectively. They show the persistence and convergence of the imaginary TA mode at the small q-vector with the supercell and k-mesh sizes. Thus, we have provided the proof of the existence of the imaginary TA mode at the small q-vector in phonon calculation for SrAl4 with two different methods in two different DFT codes using different pseudopotentials, which give the consistent results regarding q-mesh, k-mesh and supercell size convergence. We have added the following in Method section.

"In Fig.S3 we show the convergence of calculated phonon band dispersions of $SrAl_4$ with respect to increased *k*-mesh to (18×18×18) and *q*-mesh to (4×4×4) in QE using DFPT and also a larger supercell of (4×4×4) of the conventional cell with 640 atoms and increased *k*-mesh in VASP using the finite displacement method with PHONOPY."

The other important aspect to prove the existence of this imaginary TA mode for the CDW is its response to electronic smearing. As shown in Fig.4, with the change of the electronic smearing from 0.04 to 0.02 Ry, the TA mode in SrAl4 is gradually softened at the small q-vector in Fig.4(b) in a direct contrast to BaAl4. Such a distinctly different behavior can be explained by the different EPC strength in Fig.4(c)-(d), which is the key finding of our paper to reveal that the origin of the CDW (softening of the TA mode at the small q-vector) in SrAl4 and EuAl4, but not BaAl4, is due to the stronger EPC in SrAl4 and also EuAl4 (Fig.5 (e) and (g)) than BaAl4 at the small q-vector.

Reviewer #3 (Remarks to the Author):

In the manuscript by Wang, Nepal and Canfield, the authors theoretically investigate the origins of the CDW in SrAl4 and EuAl4. They calculate the electronic and phonon bandstructure using first principles and then investigate the susceptibility functions using

maximally localized Wannier functions. To understand the origins of the CDW, they consider related compounds, in particular BaAl4, that have similar crystal structure and bandstructure but no CDW. The authors find there is an enhanced electron-phonon coupling to a transverse acoustic phonon in SrAl4 and EuAl4 and a peak in the real part of the susceptibility function at the experimentally observed CDW q-vector. The authors conclude this is a stronger driving force towards the formation of the CDW than a Peierls distortion arising from imperfect Fermi surface nesting.

The manybody interactions in topological systems is a contemporary topic that appeals to a wide audience and is suitable for publication in Communication Physics. The theoretical investigation is thorough, and the conclusions are well grounded. However, I do have one concern that should be addressed prior to recommending for publication.

REPLY: We thank the reviewer for the careful reading of our manuscript and finding our work thorough and the conclusions well grounded.

The authors discuss conventional wisdom and what one should expect from the replacement of Sr with the more massive Ba ions. In summary, one should expect that BaAl4 should also form a CDW due to the heavier Ba ions. The authors then discuss how the Ba compound does not follow conventional wisdom as the electron-phonon coupling is reduced for the TA phonon responsible for the CDW formation and hence, does not exhibit a CDW. While I agree with these conclusions, I am still left wondering why. As the authors point out, the electron phonon coupling interaction has no mass dependence but evaluates changes to the deformation potential. Hence, what are these differences that deviates the behavior from the conventional wisdom. Do subtle crystal changes from the different cation sizes result in an alteration of the deformation potential observed by the electrons? Do the bulked nets of Al get altered by the different cations? If it is driven by the enhancement of the electronic phonon coupling, what is driving this enhancement? In other words, what updates to conventional wisdom can we draw from these results?

REPLY: We thank the reviewer for the suggestion. We have expanded the discussion on EPC of the TA mode in connection to the shear modulus, Poisson ratio (Table.1) and the electron charge density redistribution for the bonding between the Al network and the different cation layers (Fig.5 and also below). We find that the electron charge density redistribution can explain the different TA mode behaviors across the series of SrAl4, BaAl4 and EuAl4, which provides the important update to conventional wisdom. We have added the following two paragraphs before Conclusion.

"The TA mode CDW here involves a local shear distortion perpendicular to the *c*-axis. It is very interesting to notice that among the calculated bulk elastic properties (see Table.1), the bulk modulus (B) of 50.6 GPa for $BaAl_4$ is slightly smaller than the 52.9 GPa for $SrAl_4$, reflecting a larger cation size of Ba than Sr, giving both larger *a* and *c* lattice constants with a slightly smaller *c/a* ratio. However, the shear modulus (G) of 36.8 GPa for $BaAl_4$ is larger than the 29.1 GPa for $SrAl_4$. This corresponds to a much smaller Poisson ratio of 0.207 for $BaAl_4$ than the 0.268 for $SrAl_4$, which means a compression along the *c*-axis has a less in-plane expansion in response for $BaAl_4$ than $SrAl_4$, i.e., the

in-plane interaction is stiffer for $BaAl_4$ than $SrAl_4$. Then moving to $EuAl_4$ with the smallest lattice constants among the three, both B of 57.1 GPa and G of 33.9 GPa increase comparing to $SrAl_4$. But the G of $EuAl_4$ is still smaller than that of $BaAl_4$, resulting in a Poisson ratio of 0.252 similar to that of $SrAl_4$, not $BaAl_4$. Thus, the in-plane interaction in $EuAl_4$ is still softer than $BaAl_4$."

"To better understand these differences from electronic structure, we have plotted and compared the electron charge density difference of $\rho(XAl_4) - \rho(X) - \rho(Al_4)$ for X=Sr, Ba and Eu, respectively in Fig.5 (h-j). The charge density redistributions between the Al network and the different cation layers show that there is more electron transferred from the Ba layer to Al network and also more charge accumulation (yellow) at the boundary between the Ba and Al network than the cases of Sr and Eu. The more ionic character of the interaction in $BaAl_4$ with more in-plane charge accumulation makes it harder for the in-plane shear distortion between the Al network and Ba layer, which explains a much smaller Poisson ratio for $BaAl_4$ than $SrAl_4$ and $EuAl_4$. This also means the TA mode softening for CDW with the local shear distortion in $BaAl_4$ is much harder than that in $SrAl_4$ and $EuAl_4$. It is interesting to find the connection between the CDW with microscopic EPC interaction and the macroscopic elastic properties."

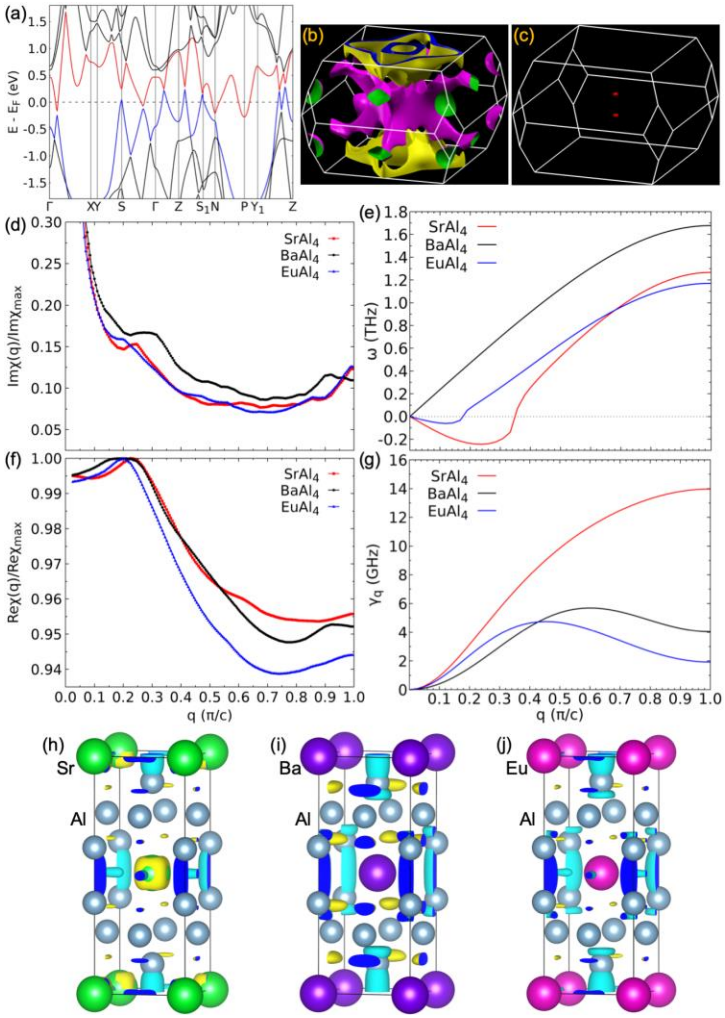

GPa	$SrAl_4$	$BaAl_4$	$EuAl_4$
Bulk modulus (B)	52.9	50.6	57.1
Shear modulus (G)	29.1	36.8	33.9
Poisson ratio (ν)	0.268	0.207	0.252

Table 1. DFT-calculated elastic properties of $SrAl_4$, $BaAl_4$ and $EuAl_4$.

Additionally, we have plotted the eigenvectors of three optical zone-center modes with sizable EPC besides the TA mode in Fig.4(e). These three modes are from Al network, namely, Eg for in-plane motion, B1g for Al1 (4d) out-of-plane motion and A1g for Al2 (4e) out-of-plane motion. Their EPC is similar to the TA mode in BaAl4, but not as strong as the TA mode in SrAl4.

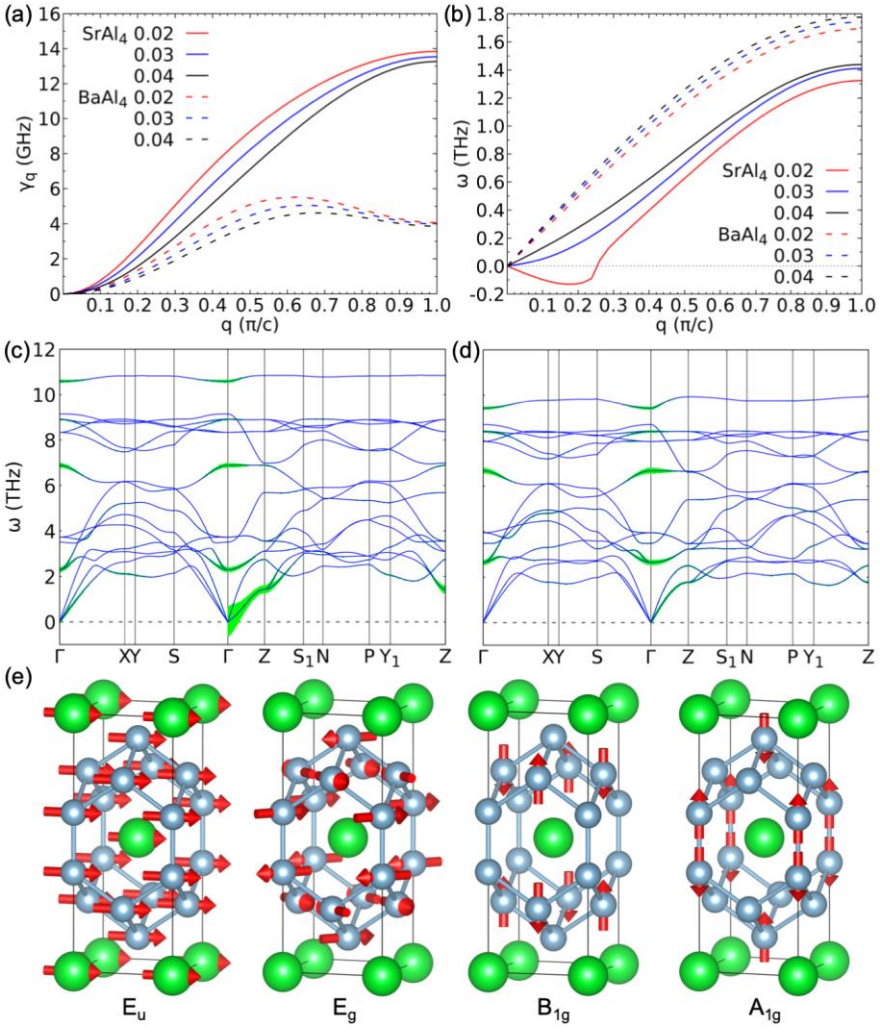

REVIEWERS' COMMENTS:

Reviewer #2 (Remarks to the Author):

In the response letter and revised manuscript, the authors have fully addressed my concerns about the controversial results between the current manuscript and the arXiv paper. They used both the finite displacement method and the DFPT method , as well as larger supercells and denser k and q grids, to prove the reliability of their conclusions. Beside, the author have also fully answered all the questions raised by other reviewers.

In this case, I do believe the authors paid great effort on this reply, and their results are solid. I support the publication of this paper in Communications Physics.

Reviewer #3 (Remarks to the Author):

The authors have carefully considered all reviewer's comments and criticisms. They have provided an extensive rebuttal with clear details for their arguments and have modified the manuscript based on the comments. I believe the authors have adequately addressed all the reviewer's concerns and recommend the manuscript for publication in its current form.